CrossMark

ORIGINAL ARTICLE

Real-time metabolomic analysis of lactic acid bacteria as monitored by in vitro NMR and chemometrics

Parvaneh Ebrahimi[1] · Flemming Hofmann Larsen[1] · Henrik Max Jensen[2] ·
Finn Kvist Vogensen[3] · Søren Balling Engelsen[1]

Abstract

Introduction Lactic acid bacteria (LAB) play an important role in the food industry as starter cultures to manufacture fermented food, and as probiotics. In recent years, there has been an increasing interest in using LAB cultures for biopreservation of food products. It is therefore of great interest to study the detailed metabolism of these bacteria.
Objectives This study aimed at developing an efficient analytical protocol for real-time in vitro NMR measurements of LAB fermentations, from sample preparation, over data acquisition and preprocessing, to the extraction of the kinetic metabolic profiles.
Method The developed analytical protocol is applied to an experimental design with two LAB strains (*Lactobacillus rhamnosus* DSM 20021 and *Lactobacillus plantarum subsp. plantarum* DSM 20174), two initial pH levels (pH$_i$ 6.5 and 5.5), two levels of glucose concentration (2.5 and 0.25 g/l), and two batch fermentation replicates.
Results The design factors proved to be strongly significant and led to interesting biological information. The

protocol allowed for detailed real-time kinetic analysis of 11 major metabolites involved in the glycolysis, pyruvate catabolism, amino acid catabolism and cell energy metabolism. New biological knowledge was obtained about the different patterns of glutamine and aspartic acid consumption by the two strains. It was observed that *L. plantarum* consumes more glutamine at low pH (pH 5.5) whereas the opposite applies to *L. rhamnosus*. Regarding aspartic acid, both of the strains consume it higher at low pH, and overall *L. plantarum* consumes it more. *L. rhamnosus* did not consume aspartic acid at pH 6.5.
Conclusion The developed analytical protocol for real-time in vitro NMR measurements of bacterial metabolism allows a relatively easy investigation of different fermentation factors such as new strains, new substrates, cohabitations, temperature, and pH and has a great potential in biopreservation studies to discover new efficient bioprotective cultures.

Keywords In vitro NMR · Lactic acid bacteria · Fermentation · Modelling metabolic profiles · Multivariate curve resolution · Reference deconvolution

✉ Parvaneh Ebrahimi
parvaneh@food.ku.dk

[1] Spectroscopy & Chemometrics, Department of Food Science, Faculty of Science, University of Copenhagen, Rolighedsvej 30, 1958 Frederiksberg, Denmark

[2] DuPont Nutrition Biosciences ApS, Edwin Rahrs vej 38, 8220 Brabrand, Denmark

[3] Food Microbiology, Department of Food Science, Faculty of Science, University of Copenhagen, Rolighedsvej 30, 1958 Frederiksberg, Denmark

1 Introduction

Lactic acid bacteria (LAB) play a very important role in food industry, and are used as starter cultures to manufacture dairy products, sourdough bread, fermented sausages, etc. (van de Guchte et al. 2002). Some of the strains of lactobacilli are used as probiotics, for which, when used as food supplements, different health benefits have been claimed (Ljungh and Wadström 2006; Kumari et al. 2011). In recent years, LAB are increasingly being used by the food industry for biopreservation, which is regarded as an

ecological solution to the problem of food spoilage and can be defined as the controlled use of antifungal and/or antibacterial microorganisms or their metabolites for the purpose of food preservation (Annou et al. 2007; Delavenne et al. 2013). There are some health concerns associated with the chemical preservatives that are commonly added to food products, whereas the use of biopreservation does not raise such concerns. However, in order to provide an efficient biopreservation system, detailed knowledge about the metabolism of the protective cultures and their responses to different environmental factors is of great importance.

Environmental metabolomics, which investigates the interactions of organisms with their environment and their response to different environmental stressors (Lankadurai et al. 2013), can be very useful in the biopreservation studies, as well as other studies that are related to the application of LAB for enhancing the sensory properties of food products. Growth and survival of bacteria that are used as biopreservatives depend upon their stress response, i.e. how they can adapt to the environmental changes such as pH, temperature, carbohydrate source concentration, other exogenous metabolites, and cell population density. Sometimes, the adaptive metabolic responses of the cells can lead to the secretion or increased production of desired antimicrobial metabolites. In fermented food products, the reroute of the bacterial metabolism under the stress condition can result in the production of more diverse metabolites, and such stress induced metabolites can in certain cases significantly enhance the sensory quality and structural properties of the food system (Serrazanetti et al. 2009). Therefore, stress conditions can be designed to augment the quality of fermented food products. In order to achieve this, a detailed understanding of the metabolism of the target microorganism and the mechanisms of stress resistance is a prerequisite. The choice of a suitable analytical platform and carefully designed experimental plans can provide this knowledge.

Nuclear magnetic resonance (NMR) spectroscopy is a powerful analytical technique that can provide valuable qualitative and quantitative information on chemical and biological samples. NMR is not selective for any special groups of chemical compounds and can with advantage be used for non-targeted analysis of biological samples. Moreover, NMR requires only simple sample preparation, is highly reproducible, is non-destructive and leaves the sample for further analysis (Emwas et al. 2013; Winning et al. 2008). ^{1}H, ^{13}C, ^{31}P and other nuclides NMR have been used widely in metabolomics studies related to human metabolism (Nicholson and Lindon 2008; Govindaraju et al. 2000; Marin-Valencia et al. 2012; Rothman et al. 2003; Rueedi et al. 2014), disease diagnostics (Emwas et al. 2013; Wang et al. 2010), and biomarker discovery

(Kim et al. 2008; Smolinska et al. 2012). Other examples include metabolomic profiling of plants (Kim et al. 2010, 2011), microorganisms (Boroujerdi et al. 2009; Grivet et al. 2003; Ramos et al. 2002; Sekiyama et al. 2011), and host-gut microbiota interactions (Nicholson et al. 2012). Proton is one of the most commonly studied nuclei and ^{1}H NMR has been increasingly used in systems biology and metabolomics (Larive et al. 2014; Nicholson and Lindon 2008; Reo 2002; Wishart 2008).

NMR has a great potential for studying living organisms, owing to its non-destructive nature, i.e. it can be used for in vivo and in vitro measurements of biological processes, with no quenching of the metabolism required. Sampling and quenching fractions of a fermentation batch is tedious and likely to introduce specific errors and irreproducibilities (Mashego et al. 2007). The real-time nature of in vivo NMR measurements prevents this problem, and NMR is the only analytical technique that can provide a vast amount of qualitative and quantitative information of the metabolome in a real-time and in vitro/vivo manner. In vitro/vivo NMR, using mainly proton, carbon, and phosphorus nuclides has been used to study microbial metabolism. For instance, ^{13}C in vivo NMR has been extensively used to investigate regulation of sugar metabolism in lactic acid bacteria (Neves et al. 1999; Ramos et al. 2002). In vivo NMR has also been used for understanding the metabolism of different carbohydrate sources by *Lactococcus lactis* (Neves et al. 2005).

One of the interesting applications of in vitro/vivo NMR has been to study the adaptive stress responses of microorganisms when they are exposed to environmental stressors. NMR can be very helpful in this context, by allowing a real-time, non-destructive and non-perturbing measurement of the rapid metabolic changes of microorganisms under the stress conditions. As an example of such a study, in vivo ^{13}C NMR has been applied to investigate how the metabolism of yeast *Saccharomyces cerevisiae* is affected by the concentration of exogenous ethanol and to model the metabolic profiles (Martini et al. 2004, 2006; Ricci et al. 2012). Other nuclides such as ^{23}Na have also been used for in vivo NMR studies of microorganisms. For example, ^{23}Na NMR spectroscopy was used to study the sugar transport and to investigate if it is sodium dependent in live *Fibrobacter succinogenes* cells (Delort et al. 2002, 2004). Despite all the advantages, one of the drawbacks of in vivo NMR is related to the heterogeneity of the samples and the presence of intracellular paramagnetic ions that can lead to the broadening of NMR signals (Grivet and Delort 2009).

This study presents an efficient analytical protocol for real-time in vitro ^{1}H NMR analysis of bacterial fermentations, and an effective solution to the inherent inhomogeneity of in vitro NMR measurements of cells. The

protocol is applied to an experimental design with two strains of LAB, *Lactobacillus rhamnosus* DSM 20021 and *Lactobacillus plantarum* subsp. *plantarum* DSM 20174 (hereafter, *L. plantarum*), two initial pH (pH_i) values and two levels of glucose concentration of a chemically defined medium. The kinetic profiles of selected metabolites are modeled by multivariate curve resolution alternating least squares (MCR-ALS) analysis (Lawton and Sylvestre 1971; de Juan et al. 2014), or by using the second order derivative of the signal. The time-series data were processed with reference deconvolution (Morris et al. 1997; Morris 2007; Ebrahimi et al. 2014) for lineshape enhancements and correcting the broadening of the NMR signals during fermentation, and *i*coshift (Savorani et al. 2010) was used for spectral alignment. The results of the experimental design are further analyzed by ANOVA-simultaneous component analysis (ASCA) (Smilde et al. 2005), and metabolite–metabolite correlations presented in heat maps.

2 Materials and methods

In this section, the experimental design and procedure, as well as the data acquisition, processing and analysis are presented. In the last subsection, some theory and background on the relevant metabolism of lactic acid bacteria are presented.

2.1 Experimental design and sample preparation

The experimental design of the study includes two strains of LAB, *L. rhamnosus* DSM 20021 and *L. plantarum* DSM 20174, two levels of glucose concentration, 2.5 and 0.25 g/l, and two initial pH (pH_i) values, 6.5 and 5.5 (See Fig. 1S, the Online Resource). The goal was to investigate how the fermentation and the metabolism of the bacteria are influenced by the design factors, and discover some of the biological differences between the strains. In order to avoid the full repetition of the names of the samples in the paper, the following abbreviations were used: 'R' for *L. rhamnosus,* 'P' for *L. plantarum,* 'GH' for samples with high glucose concentration, and 'GL' for samples with low glucose concentration. As an exmaple, 'R6.5GH' refers to the *L. rhamnosus* samples with pH_i 6.5 and high glucose concentration. The abbreviations for the samples names are listed in Fig. 1S (the Online Resource). The strains were obtained from Leibniz Institute DSMZ-German Collection of Microorganisms and Cell Cultures (DSMZ, Braunschweig, Germany). Chemically defined interaction medium (CDIM) was prepared as described previously (Aunsbjerg et al. 2015), but glucose and lactate were excluded, and this CDIM was used as the growth medium for the bacteria. All the chemicals that were used to prepare

the CDIM and the samples were obtained from Sigma-Aldrich (Schnelldorf, Germany). Water that was used for preparing the CDIM was freshly produced Milli-Q quality (Merck Millipore, Billerica, MA, USA) water. The same batch of the CDIM was used for all the samples. Phosphate buffer was prepared with pH 6.5 (0.15 M and the buffer capacity of 0.09), and pH 5.5 (0.5 M and the buffer capacity of 0.10). The buffers were used to adjust the pH of the CDIM to 6.5 and 5.5, and glucose was added to make the two glucose levels of the design. The prepared CDIM were filter-sterilized by 0.2 μm pore size filter (Nalgene®, Thermo Fisher Scientific Inc., Waltham, MA, USA), before storage in the freezer and also prior to use in the experiments. The strains were stored in Ringer solution with 10 % v/v glycerol at −80 °C until use. Before inoculating the CDIM, the cells were centrifuged for 15 min at $6000 \times g$ and 4 °C and washed with CDIM twice, to wash out glycerol and avoid its signals in the ^1H NMR spectra, as they can overlap with the signals of interest. Then, the cell pellets were used to inoculate CDIM with 10^7 CFU/ml. Deuterated water (D_2O) containing 0.1 % 4,4-dimethyl-4-silapentane-1-sulfonic acid (DSS) was sterilized by 0.2 μm pore size syringe filters (Minisart®, Sartorius, Goettingen, Germany) prior to sample preparation. DSS signal served as an internal reference for the calibration of chemical shift axis. The samples were prepared by adding 1200 μl of CDIM and 300 μl of D_2O/DSS solution to the cell pellets after the wash. For in vitro measurements, 1 ml of the samples was put in autoclave sterilized NMR tubes. To follow the cell growth in parallel, 200 μl of each sample was put in 96-well plates, besides 200 μl of the pure cell-free CDIM as reference, both in duplicates, to measure optical density (OD) during the fermentation. For all of the 8 samples in the design, duplicate samples were prepared and analyzed by this procedure.

2.2 Data acquisition and data processing

The sample in the tube was fermented inside the magnet of the NMR spectrometer at 37 °C (310 K) for 24 h, and ^1H NMR spectra of the sample were recorded every 14 min, resulting in 102 spectra for each experiment. The spectrometer was a Bruker Avance-III 600 spectrometer (Bruker Biospin Gmbh, Rheinstetten, Germany) operating at a proton frequency of 600.13 MHz (14.1 T), using a double-tuned TCI probe (cryoprobe) equipped for 5 mm sample tubes. All the spectra were recorded using the 'noesygppr1d' pulse sequence, employing a spectral width of 20 ppm, a recycle delay of 10 s, and 64 scans. Taking the duplicates into account, the final acquired NMR data consisted of 16 data matrices, having 102 spectra in the rows and the ppm variables in the columns. The processing

of the data, including phase correction, apodization, Fourier transformation, baseline correction, referencing to DSS signal, and reference deconvolution, was performed using the DOSY Toolbox (Nilsson 2009). For reference deconvolution, DSS singlet and a 5 Hz Gaussian target lineshape were used.

Reference deconvolution is a post-measurement NMR data processing method that can correct systematic errors in NMR spectra. It is previously shown by designed artificial 'metabolic' experiments that reference deconvolution can be helpful in improving the multivariate analysis results of NMR data, by enhancing the line-shapes and bi-linearity of the signals (Ebrahimi et al. 2014). In this work, reference deconvolution was used to solve the line broadening problem of the in vitro fermentations, and thus to preserve the bi-linearity of the data. The latter is a pre-requisite for application of methods such as multivariate curve resolution alternating least squares (MCR-ALS) (Engelsen et al. 2013).

The data was then imported into MATLAB 2013b (MathWorks, Inc., Natick, MA, USA), and further processed by normalizing the spectra relative to the DSS signal area. Then, the icoshift program (Savorani et al. 2010) was used to align the signals, first relative to the DSS signals and then in the defined intervals, which included the signals of interest. For a few signals such as acetate, perfect alignment could not be achieved due to large shifts of the signals between the samples with the different pH_i values. As the last preprocessing step, and prior to multivariate data analysis, spectral regions containing resonances only from noise, water, or DSS were excluded from the data.

The OD of the samples in the 96-well plates were measured at 600 nm, automatically every 14 min, in parallel with the in vitro NMR measurements, by a Multiskan[TM] FC Microplate photometer (Thermo Scientific Inc., Waltham, MA, USA). The plates were shaken by the instrument for 2 s before each reading. Only 100 readings were possible for each experiment, as it was the maximum allowed number of readings for each time-series measurement on the photometer. The OD curves where plotted by averaging the OD values of the duplicate wells of each sample that were measured by the photometer, and subtracting the mean OD value of the CDIM.

2D NMR spectra (including correlation spectroscopy (COSY), total correlation spectroscopy (TOCSY), ^{1}H-^{13}C heteronuclear single-quantum correlation spectroscopy (^{1}H-^{13}C HSQC), and ^{1}H-^{13}C heteronuclear multiple-bond correlation spectroscopy (^{1}H-^{13}C HMBC) of some of the ferments at the endpoint of the fermentation were recorded to support assignments of the resonances; these data were not used in the data analysis. The signals were assigned by using human metabolome database (HMDB) (Wishart

et al. 2007, 2009, 2012), and biological magnetic resonance bank (BMRB) (Ulrich et al. 2008) databases.

2.3 Data analysis

2.3.1 Extracting the metabolic profiles

Kinetic metabolic profiles were extracted by using multivariate curve resolution-alternating least squares (MCR-ALS) algorithm (de Juan et al. 2014) on spectral intervals containing the signals that were well-aligned between the spectra, or by modeling the minimum of the peaks second derivative for (singlet) resonances that could not be aligned by icoshift (Savorani et al. 2010), because of the considerable shift or concentration difference between the samples. For MCR-ALS modeling, MCR-ALS graphical user interface (GUI) was used (Jaumot et al. 2005). Non-negativity constraints were applied on both the spectral and concentration (time) profiles. As the initial concentrations of the nutrients in the CDIM were known, their profiles were scaled accordingly.

2.3.2 Heat maps and ASCA

Pearson correlation coefficients were calculated between the kinetic profiles of the metabolites in each sample (duplicates were averaged). In order to focus on the significant correlations, the coefficients less than -0.8 were set to -1, and the coefficients greater than $+0.8$ were set to $+1$. The coefficients that were in-between were all set to zero. Correlation coefficients are shown in heat maps that are colored by the value of the coefficients.

Analysis of variance-simultaneous component analysis (ASCA) (Smilde et al. 2005) was performed on the extracted metabolic profiles and the OD profiles, excluding lactate and glucose profiles, by using an in-house MATLAB code. The null hypothesis was tested for the main and interaction ASCA effect matrices by a permutation test with 50,000 permutations, in order to evaluate the statistical significance as expressed in the p-values. Some of the resulting effect matrices were analyzed further by principal component analysis (PCA). Prior to the PCA, the residual matrix was added to the effect matrices and autoscaling was used.

2.4 Metabolism of lactic acid bacteria

Figure 1 shows homolactic fermentation (glycolysis pathway) in which pyruvate and subsequently lactate are produced from glucose. The transfer of a phosphate group from phosphoenolpyruvate (PEP) to ADP, which is catalyzed by pyruvate kinase (PK, [EC: 2.7.1.40]), yields
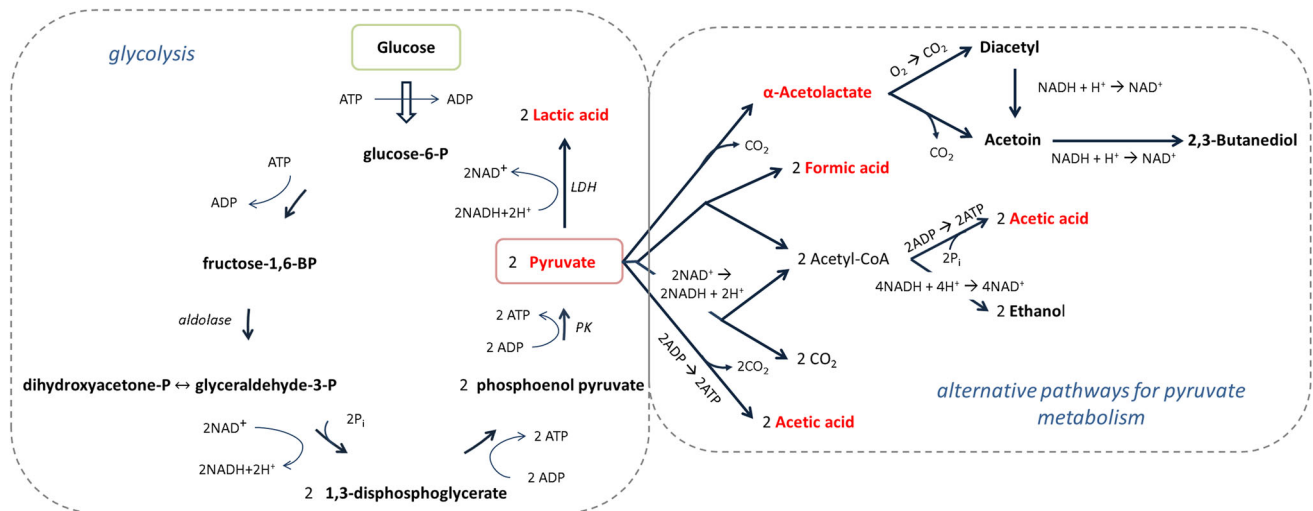
Fig. 1 Glycolysis (Embden–Meyerhof–Parnas pathway) and the alternative routes for pyruvate catabolism. The metabolites that are written in *red* are among the metabolites that were identified by the in vitro NMR measurements of the experimental design samples (Color figure online)

one molecule of pyruvate and one molecule of ATP. This reaction is identified as one of the bottlenecks in glycolysis, at least under the circumstances of limiting glucose concentration. It is suggested that after the addition of glucose or close to its depletion, the high concentration of intracellular inorganic phosphate, P_i, leads to the reduced activity of PK and as a result the accumulation of PEP and the formation of a metabolic bottleneck at this level (Neves et al. 2005; Kowalczyk and Bardowski 2007). However, it seems that it is not only a single enzyme, but rather many different enzymes that control the glycolytic flux (Koebmann et al. 2002).

Pyruvate can be reduced to lactic acid, through the reaction:

$$pyruvate + NADH + H^+ \leftrightarrow lactate + NAD^+$$

catalyzed by lactate dehydrogenase (LDH, [EC: 1.1.1.27] and [EC: 1.1.1.28] for the *L* and *D* enantiomers)) (Hung and Yellen 2014). NAD is an important cofactor for some of the reduction–oxidation reactions in biochemical processes such as glycolysis. The cytosolic free ratio of $NADH/NAD^+$ determines the redox state of the cell and is important to keep the redox balance in the cell during glycolysis. It is suggested that $NADH/NAD^+$ can regulate glycolysis by affecting the activity of involved enzymes such as LDH (Neves et al. 2005). Accordingly, the ratio of lactate/pyruvate is regulated by the redox state of the cell according to the above biochemical reaction, and $NADH/NAD^+$ ratio is the main factor that controls how much of the metabolized pyruvate is reduced to lactate during glycolysis (Hung et al. 2011; Sun et al. 2012).

Depending on the type of the bacteria and the physiological conditions, pyruvate can be converted into other metabolites than lactate, through other biochemical pathways. In this metabolism that is known as mixed-acid fermentation, acetic acid, formic acid, succinic acid, and also ethanol can be produced in addition to lactic acid. A higher $NADH/NAD^+$ ratio stimulates higher LDH activity and consequently promotes homolactic metabolism and higher lactate formation from pyruvate. On the other hand, a lower $NADH/NAD^+$ ratio reduces the activity of LDH and shifts the metabolism towards mixed-acid fermentation (Kowalczyk and Bardowski 2007). Some of the alternative pathways for pyruvate consumption through mixed-acid fermentation are shown in Fig. 1. Acetic acid is one of the important metabolites that pyruvate can be converted to. Pyruvate dehydrogenase [EC: 1.2.4.1] can convert pyruvate to acetyl-CoA and subsequently acetate kinase [EC: 2.7.2.1] can catalyze the production of acetate from acetyl-P. The activity of pyruvate oxidase [EC: 1.2.3.3] can also lead to the production of acetate from pyruvate. Pyruvate can also be converted to α-acetolactate by acetolactate synthase (ALS, [EC: 2.2.1.6]) (Lahtinen et al. 2011), which according to the pathways shown in Fig. 1, can be subsequently converted to diacetyl and acetoin. Acetolactate is converted to diacetyl through a non-enzymatic chemical oxidation with the release of CO_2, and diacetyl can be subsequently reduced to acetoin by diacetyl reductase ([EC: 1.1.1.303] and [EC: 1.1.1.304], for the *R* and *S* configurations). Acetolactate can also be directly converted into acetoin by α-acetolactate decarboxylase [EC: 4.1.1.5] (Caspi et al. 2014). Synthesis of α-acetolactate is active only under the condition of surplus pyruvate, and will be enhanced at low pH values (Le Bars and Yvon 2008). By mixed-acid fermentation pyruvate can also be converted into formic acid. This pathway is catalyzed by pyruvate

formate lyase [EC: 2.3.1.54], which is highly sensitive to oxygen.

Metabolism of amino acids by LAB have important physiological roles including intracellular pH control, controlling the redox state of the cells, and being involved in metabolic stress responses. As LAB are widely used for the production of fermented food products by the industry, studying the catabolism of amino acids by LAB is relevant for the safety and the quality of fermented products. Studying the metabolism of amino acids by LAB has received special attention, because the products from amino acids catabolism can significantly enhance the sensory properties of food products. It is previously reported that for many of LAB strains, catabolic pathways of amino acids start with transamination, which requires presence of α-ketoglutarate (Amarita et al. 2001; Helinck et al. 2004). LAB strains that have active glutamate dehydrogenase (GDH, [EC: 1.4.1.2]) can produce α-ketoglutarate from deamination of glutamic acid, by the biochemical reaction (Tanous et al. 2002):

$$\text{glutamate} + \text{NAD}^+ \overset{GDH}{\leftrightarrow} \alpha\text{-ketoglutarate} + \text{NADH} + \text{H}^+$$
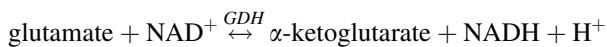
As catabolism of amino acids can produce aromatic compounds, especially from the aromatic, branched-chain and, sulfur-containing amino acids, strains that have higher activity of GDH can be used for flavor enhancement in food products (Kieronczyk et al. 2003; Helinck et al. 2004; Liu et al. 2008). Amino acids can also be used as energy sources, or be involved in the pathways regarding cells stress responses (Fernández and Zúñiga 2006). There is not detailed knowledge on the catabolism of glutamine by LAB, but it has been observed that several strains of LAB can metabolize it (Kieronczyk et al. 2001; Williams et al. 2001). For aspartic acid, three catabolic pathways have been reported that are catalyzed by three different enzymes: aspartate aminotransferase [EC: 2.6.1.1], aspartate ammonia-lyase [EC: 4.3.1.1], and aspartate decarboxylase [EC: 4.1.1.11]. The pathway catalyzed by the aspartate aminotransferase produces oxaloacetate and pyruvate, the one catalyzed by aspartate ammonia-lyase, depending on the conditions can produce fumaric acid, succinic acid or malic acid, and finally the pathway catalyzed by aspartate decarboxylase can synthesize alanine (Fernández and Zúñiga 2006).

Nucleosides are very important endogenous metabolites in LAB, as they are used as the building blocks of DNA and RNA after phosphorylation and forming nucleotides. They also serve a very important role in cells energy metabolism. Some bacteria can use nucleosides as carbon source by degrading their pentose ring. Moreover, it is reported that adenosine may be utilized as nitrogen source without degradation of purine ring

(Kilstrup et al. 2005). To metabolize adenosine as a purine source, it should be deaminated by adenosine deaminase (ADD, [EC: 3.5.4.4]) to yield inosine. Inosine can then undergo phosphorolytic cleavage, generating ribose-1-P and hypoxanthine, catalyzed by purine nucleoside phosphorylase (PNP, [EC: 2.4.2.1]), according to the following reaction:

$$\text{inosine} + \text{P}_i \overset{PNP}{\leftrightarrow} \text{hypoxanthine} + \text{ribose-1-phosphate}$$
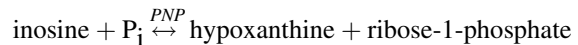
PNP can also convert adenosine into adenine (Kilstrup et al. 2005).

3 Results and discussion

3.1 The time-series NMR spectra and the extraction of the metabolic profiles

When the number of cells increases during fermentation, the samples can become inhomogeneous because of the cells coagulation. The inhomogeneity in the sample will result in line broadening of the signals in the NMR spectra towards the end of the fermentations. Therefore, for a time-series measurement of fermentation, signals will get broader during the fermentation, as long as the cells are propagating. Lineshape changes by time will definitely lead to errors in quantitative multivariate analysis of the metabolic changes of such data, by methods like principal component analysis (PCA), partial least squares (PLS) regression, and multivariate curve resolution-alternating least squares (MCR-ALS) that have bilinearity of the data as their main principle. Reference deconvolution was used on the data, in order to enhance the quality of the spectra and to solve the line broadening problem.

Figure 2 shows some of the resonances from one of the time-series spectra processed with and without reference deconvolution with a 5 Hz Gaussian target lineshape, and subsequently aligned by *i*coshift program. As can be observed from the figure, reference deconvolution significantly improves the quality of the spectra, and the lineshapes become more consistent between the spectra after applying this method, which in turn makes the data more suitable for bilinear modelling. Moreover, Fig. 2 shows that using *i*coshift on reference-deconvoluted data corrects the shifts in the position of the resonances between the spectra. This will also lead to the improved multivariate data analysis results. To our knowledge, this is the first application of reference deconvolution to improve the multivariate analysis results of real metabolomics data. In any further analysis of the data and modeling the metabolic profiles, the reference deconvoluted and *i*coshifted data was used.
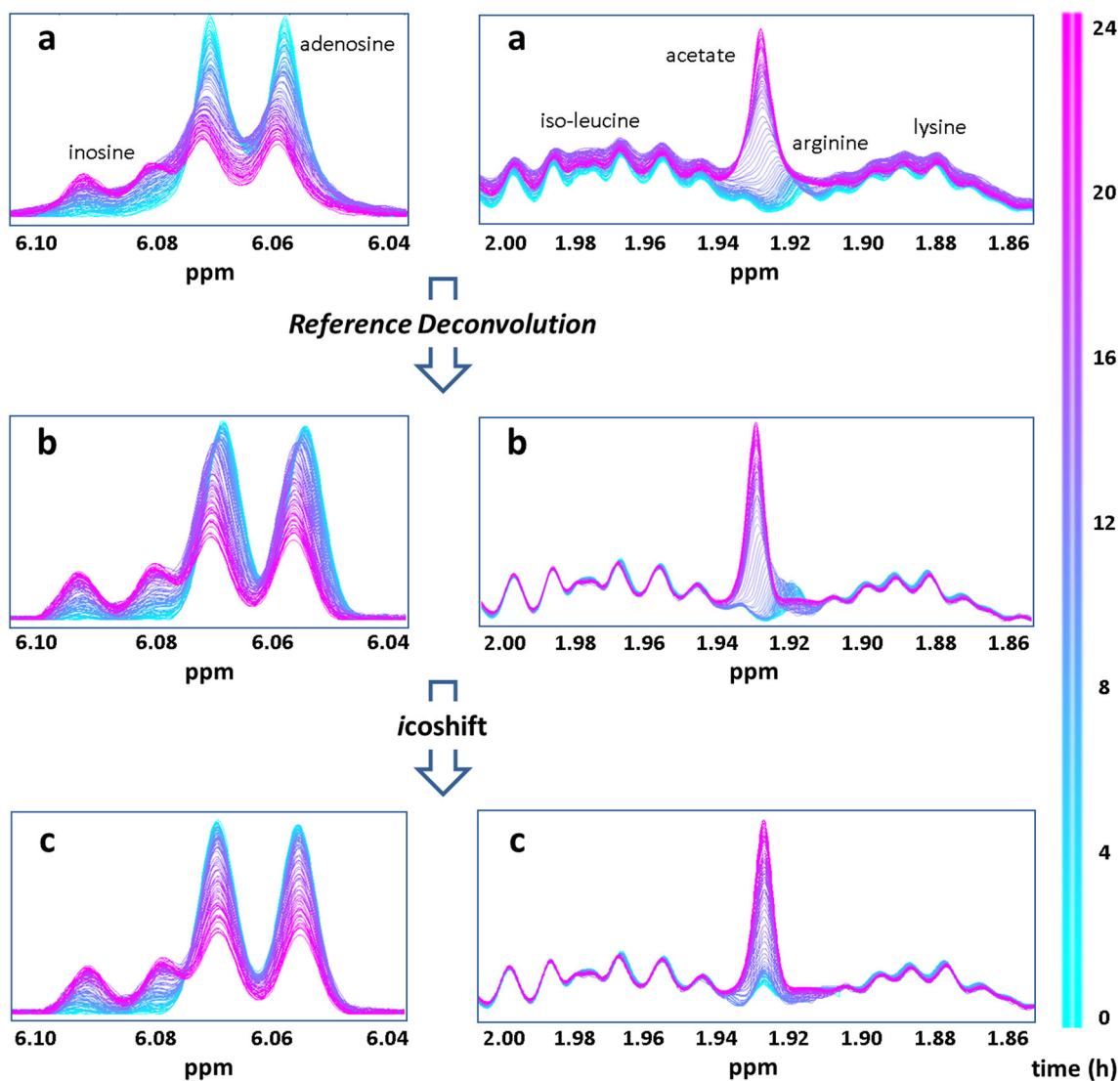
Fig. 2 Enhancing the quality of real-time in vitro measurements of bacterial fermentation by reference deconvolution and *i*coshift. Reference deconvolution can enhance the lineshapes consistencies and correct line broadening, and *i*coshift can align the resonances and correct the shifts in peaks position; **a** original time-series data, **b** reference deconvoluted data, and **c** reference deconvoluted and aligned data

Table 1 lists the metabolites that were observed to change during fermentation, as measured by ^{1}H NMR. It also shows the specific resonances of each metabolite that was used for extracting the kinetic profiles, and the method that was applied for this purpose (see Sect. 2.3). The NMR signals of the modeled metabolites in one of the 'R5.5GH' time-series are shown in Fig. 2S (the Online Resource). As adenosine and inosine signals overlap slightly, one MCR-ALS model with two components was used to model the profiles of both signals simultaneously. Besides, as inosine signal shifts between the samples with pH$_i$ 6.5 and 5.5, models were calculated for the two pH$_i$ values separately.

3.2 Cell growth and substrate depletion

The extracted metabolic profiles, as well as the OD curves are presented in Fig. 3. To avoid repetition of the samples names, abbreviations that are defined in Sect. 2.1 and Fig. 1S (the Online Resource) will be used for discussing the profiles. The OD curves (Fig. 3a) show that cells grow more rapidly in samples with pH$_i$ 6.5, and in samples with the high glucose concentration. Cell growth (OD values) is lower in all samples with pH$_i$ 5.5, and this effect is more pronounced in *L. plantarum* samples. According to the glucose profiles (Fig. 3b, c), *L. plantarum* depletes glucose faster in samples with high glucose concentration, whereas

Table 1 List of the modeled metabolites, the specific signal that was used for extracting the profiles, and the modelling approach that was applied

Metabolites	NMR signal	Signal type	Profile extracting approach
Glucose	5.23 ppm	Doublet	MCR-ALS
Lactate	1.32 ppm	Doublet	MCR-ALS
Pyruvate	2.36 ppm	Singlet	2nd derivative
Acetic acid	1.91 ppm (pH 6.5); 1.94 ppm (pH 5.5)	Singlet	2nd derivative
α-Acetolactate	1.50 ppm (pH 6.5); 1.51 ppm (pH 5.5)	Singlet	2nd derivative
Formic acid	8.46 ppm	Singlet	MCR-ALS
Glutamine	2.45 ppm	Doublet of doublet	MCR-ALS
Aspartic acid	2.70 ppm	Doublet of doublet	MCR-ALS
Adenosine	6.06 ppm	Doublet	MCR-ALS (separately on pH 6.5 and pH 5.5 datasets)
Inosine	6.08 ppm (pH 6.5); 6.09 ppm (pH 5.5)	Doublet	MCR-ALS (separately on pH 6.5 and pH 5.5 datasets)
Adenine	8.20 ppm (pH 6.5); 8.22 ppm (pH 5.5)	Singlet	2nd derivative

in samples with low glucose concentration, *L. rhamnosus* depletes glucose faster. In the beginning of the fermentation *L. rhamnosus* consumes glucose faster, but since *L. plantarum* continuously increases its glucose consumption rate, it overhauls *L. rhamnosus* towards the end of the fermentation process. The rate of glucose consumption decreases in the low pH_i value and this affects *L. rhamnosus* more than *L. plantarum*. Both of the studied strains can obtain energy from glucose through the glycolysis pathway, which is shown in Fig. 1.

3.3 The homofermentative pathway and mixed-acid fermentation

Pyruvate is a key metabolite in the homofermentative pathway where it is converted to lactate as the main metabolic end-product. Figure 3d, e show the kinetic profiles of lactate, for high and low glucose concentration, respectively. For both strains, a higher amount of lactate is produced and more pyruvate is accumulated at pH_i 6.5 samples compared to pH_i 5.5 samples. This difference can be explained by the difference in the intracellular pH. At pH 6.5, the intracellular pH is close to neutral ($\sim$7.5), whereas at pH 5.5, the intracellular pH is close to 6.5 (Siegumfeldt et al. 2000). This leads to the higher activities of PK and LDH (the two enzymes that catalyze the production of pyruvate and lactate respectively) in samples with pH_i 6.5, in which the intracellular pH is closer to the optimum pH of the enzymes activity. In addition, the activity of LDH seems to be higher in *L. plantarum* samples, as higher amount of lactate is produced in these samples (Fig. 3d, e). On the other hand, as Fig. 3f shows, more pyruvate is accumulated in *L. rhamnosus* samples, which can result from the lower activity of LDH that converts pyruvate to lactate. According to Fig. 3e, for

'P6.5GL' and 'P5.5GL' samples, the patterns of the lactate profiles are different from the other samples. In 'P5.5GL', the concentration of lactate increases slightly even after glucose depletion, whereas it remains constant in the other samples. According to the extracted metabolic profiles, after glucose depletion (see Fig. 3b), pyruvate concentration decreases in samples with the higher glucose concentration (see Fig. 3f). However, this decrease is not observed in samples with low glucose concentration. Samples with the lower glucose concentration have a lower metabolic flux and NADH/NAD$^+$ ratio, which as discussed earlier in Sect. 2.4 can lead to the reduced activity of enzymes that are involved in the conversion of pyruvate to other metabolites. (Koebmann et al. 2002).

Figure 3g shows the kinetic profiles of acetic acid, which is one of the metabolites that pyruvate can be converted to through mixed-acid fermentation. As the profiles show all the design factors affect the formation of acetic acid. Overall, *L. plantarum* samples produce more acetic acid than *L. rhamnosus* samples, and its highest yield is observed in 'P6.5GL' samples (Fig. 3g). Amongst the *L. rhamnosus* samples, the highest acetic acid was achieved at pH_i 6.5 and low glucose concentration. The higher production of acetic acid in samples with the low glucose concentration can be explained by the smaller NADH/NAD$^+$ ratio in these samples that shifts the fermentation towards mixed-acid fermentation. Besides, among the samples with the low glucose concentration, the activity of acetate kinase [EC: 2.7.2.1] is higher in samples with pH_i 6.5 that leads to a higher production of acetate (Fig. 3f). In a similar way, the lower production of acetate in samples with high glucose concentration is related to the higher NADH/NAD$^+$ ratio in these samples that stimulates homolactic fermentation. In samples with high glucose concentration, formation of acetic acid is increased close to

or after glucose depletion, whereas in samples with low glucose concentration, acetic acid is formed already from the beginning of the fermentation. This trend is observed by comparing the acetic acid profiles of 'P6.5GL' and 'P6.5GH' samples (Fig. 3g), for instance. In samples with high glucose concentration, close to the depletion of glucose, the reduced $NADH/NAD^+$ ratio stimulates mixed-acid fermentation, whereas in the samples with low glucose concentration the small $NADH/NAD^+$ ratio from the beginning of the fermentation shifts the metabolism towards mixed-acid fermentation.

Figure 3h shows the kinetic profiles of α-acetolactate. α-Acetolactate can be produced from pyruvate in mixed-acid fermentation, catalyzed by acetolactate synthase (ALS, [EC: 2.2.1.6]). According to the α-acetolactate profiles (Fig. 3h), α-acetolactate is accumulated only in *L. rhamnosus* samples, at least to a concentration that is detectable by ^{1}H NMR. However, according to Kyoto Encyclopedia of Genes and Genomes (KEGG) (Kanehisa and Goto 2000) both of the strains have ALS genes. The reason that α-acetolactate is accumulated and observed in only one of the strains may be attributed to the difference in the activity of ALS, diacetyl reductase ([EC: 1.1.1.303] and [EC: 1.1.1.304], for the *R* and *S* configurations), or α-acetolactate decarboxylase [EC: 4.1.1.5] between the strains. The highest concentration of this metabolite is produced in 'R5.5GH' samples, which have high amount of accumulated pyruvate and also a lower pH value—the two factors that enhance the production of α-acetolactate (Le Bars and Yvon 2008). 'R6.5GL' samples produce the lowest amount of α-acetolactate, which can be explained by the same reasoning. A considerable decline in the concentration of α-acetolactate is observed in 'R5.5GH' samples after glucose depletion (Fig. 3h), which implies that diacetyl or acetoin are produced. However, signals from acetoin and diacetyl could not be identified, presumably due to their low concentration. It is previously reported that for *L. lactis,* under the condition of surplus pyruvate, at pH 5.0 α-acetolactate was mainly converted into diacetyl, whereas between pH 5.5 and 7.0, it was mainly converted into acetoin (Le Bars and Yvon 2008). Diacetyl and acetoin are redox pairs, and depending on the free $NADH/NAD^+$ ratio in the cells, and also activity of diacetyl reductase, the ratio of the diacetyl that is reduced to acetoin can vary. Activity of α-acetolactate decarboxylase also affects the rate of the direct conversion of α-acetolactate into acetoin. The extracted α-acetolactate profiles are not as reproducible as the other profiles for the duplicates. This can be explained by the fact that α-acetolactate is highly unstable and in the presence of oxygen will be quickly converted to diacetyl, and under anaerobic condition it can be converted to acetoin.

Figure 3i shows the formic acid profiles. Pyruvate can be converted to formic acid by pyruvate formate lyase [EC: 2.3.1.54]. Only 'R5.5GH' and 'P5.5GH' samples produce formic acid according to the profiles, with the highest amount being produced by 'R5.5GH'. The other samples do not produce detectable amount of formic acid. Accordingly, it can be concluded that pyruvate formate lyase is active in the low pH value, pH_i 5.5, and when there is higher amount of carbohydrate source present, and under these conditions, it is more active in *L. rhamnosus* samples.

3.4 The catabolic pathways of amino acids

The kinetic profiles of glutamine catabolism are shown in Fig. 3j. According to KEGG, both of the studied strains have GDH (Kanehisa and Goto 2000). When examining the extracted metabolic profiles for glutamine (Fig. 3j), *L. plantarum* samples consume higher amount of glutamine compared to the *L. rhamnosus* samples. Besides, in *L. plantarum* samples, the consumption of glutamine is higher at pH_i 5.5 than at pH_i 6.5 (Fig. 3j). For *L. rhamnosus* samples, 'R6.5GH' and subsequently 'R5.5GH' consume the highest amount of glutamine. For both *L. plantarum* and *L. rhamnosus*, more glutamine is consumed in samples with the higher glucose concentration. For samples with the lower glucose concentration, glutamine is consumed to a much lower extent, with 'R5.5GL' samples being the lowest (Fig. 3j). As glutamine, after being converted to α-ketoglutarate, plays a role in the catabolism of amino acids by starting the transamination step as the amino group acceptor, augmenting its consumption can benefit the catabolism of amino acids. This can be of high interest for enhancing the sensory properties of food products, as the catabolism of some amino acids can lead to the formation of desirable aroma compounds. For this purpose, the application of the strains that have high GDH activity and also optimizing influential parameters like pH for increasing glutamine consumption will be helpful. The extracted kinetic profiles of glutamine provide interesting information about the efficiency and the differences of the two investigated strains in metabolizing glutamine. It is observed that *L. plantarum* consumes more glutamine than *L. rhamnosus* (Fig. 3j), which can be attributed to the higher activity of GDH in *L. plantarum*. Another interesting observation was the contradictory effect of pH on the consumption of glutamine by the two strains; for *L. plantarum,* the low pH value (pH_i 5.5) enhances glutamine consumption, whereas for *L. rhamnosus* samples, consumption of glutamine is higher at pH_i 6.5 (Fig. 3j). This information can be very helpful when these strains are used in food products. Resonances from the catabolic products of glutamine were not sufficiently intense to be identified reliably by ^{1}H NMR.
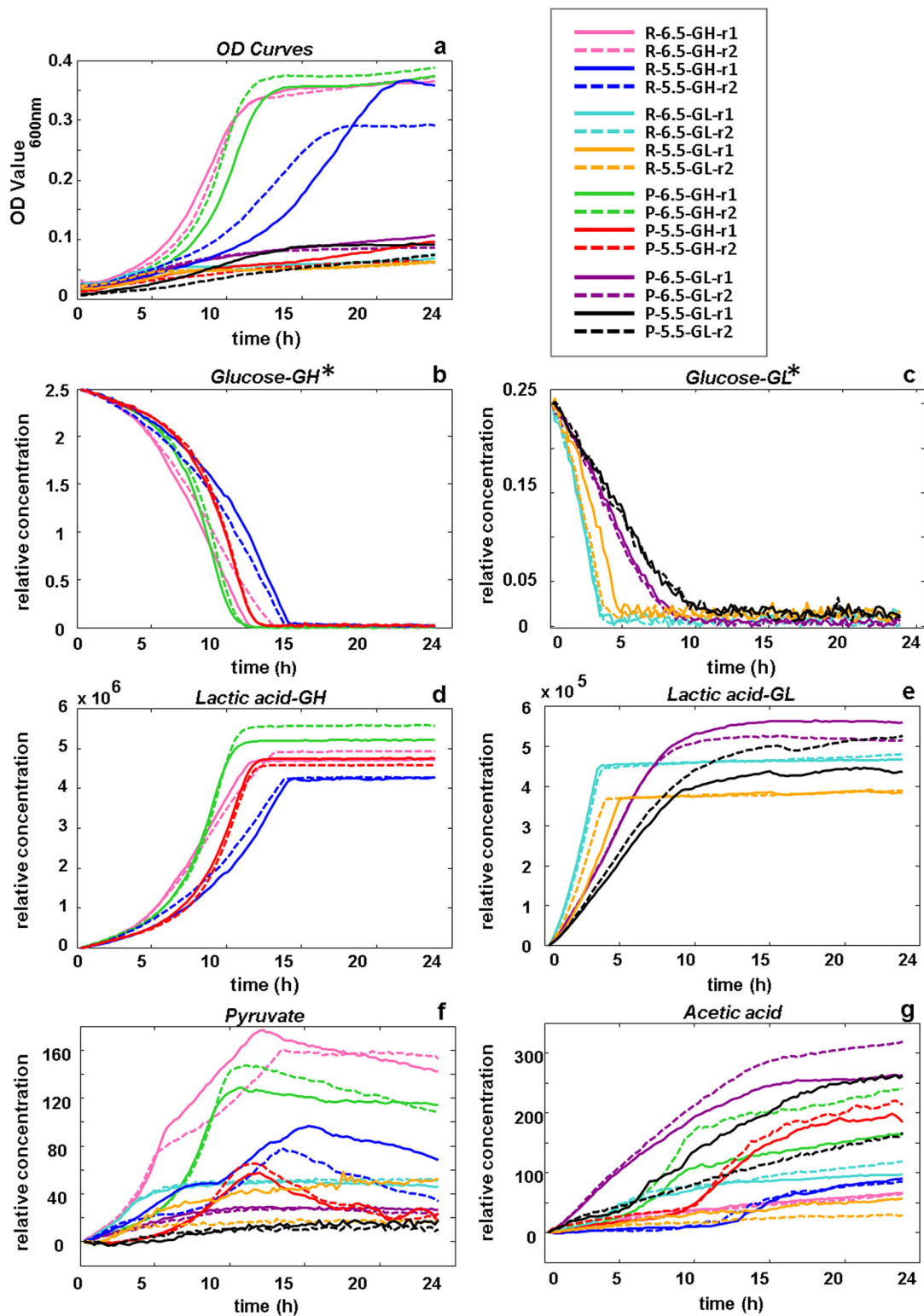
Fig. 3 The calculated metabolic profiles and the optical density curves. The profiles that are marked with the asterisk are scaled using their initial concentration in the CDIM; **a** optical density curves, **b** and **c** glucose profiles for samples with high and low glucose content respectively, **d** and **e** lactic acid profiles for samples with high and low glucose content respectively, **f** pyruvate profiles, **g** acetic acid profiles, **h** α-acetolactate profiles, **i** formic acid profiles, **j** glutamine profiles, **k** aspartic acid profiles, **l** adenosine profiles, **m** inosine profiles, and **n** adenine profiles
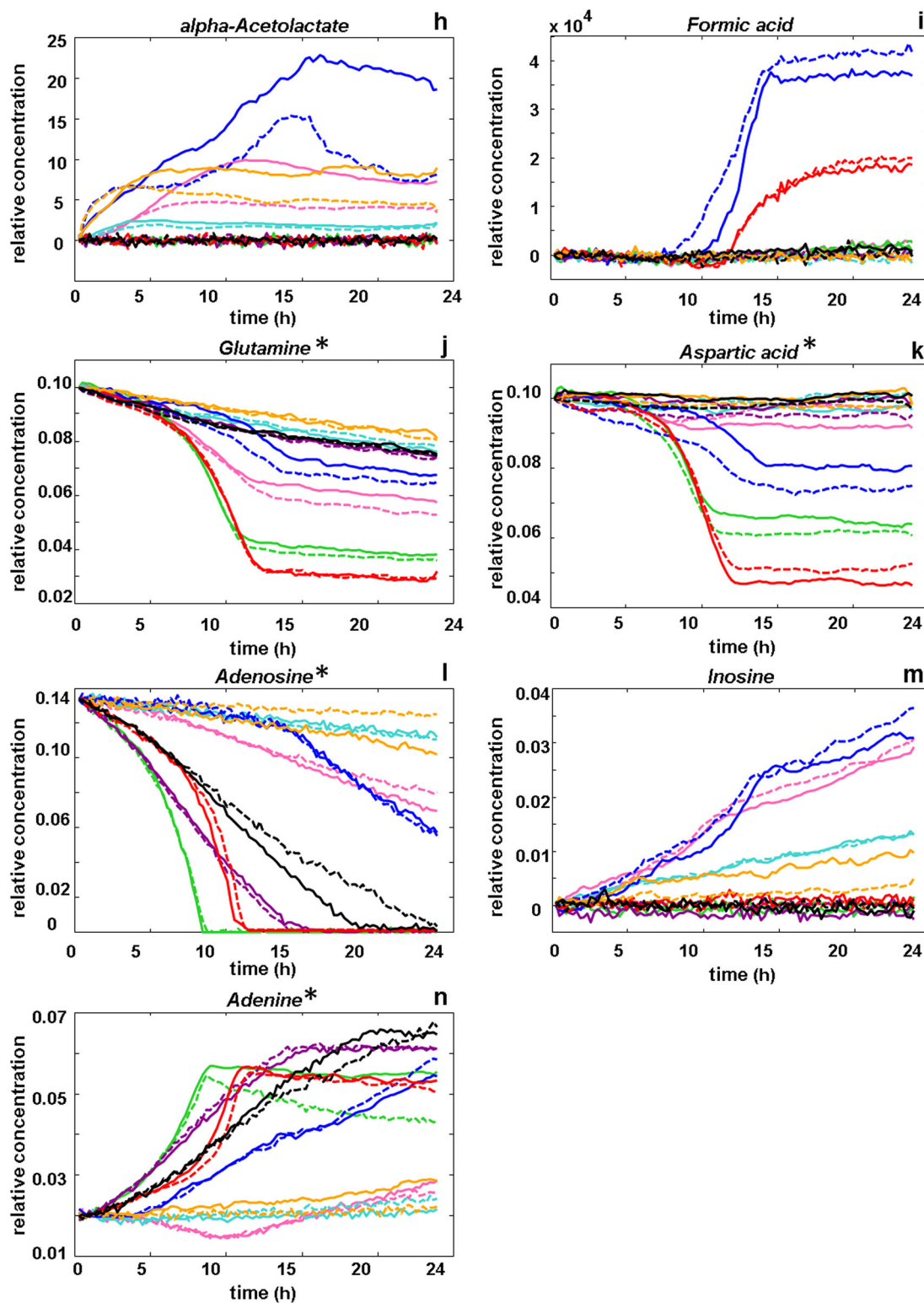
Fig. 3 continued

The kinetic profiles of aspartic acid catabolism are shown in Fig. 3k. According to KEGG (Kanehisa and Goto 2000) both of the studied strains have aspartate ammonia-lyase [EC: 4.3.1.1], which suggests that they can consume aspartic acid and produce fumaric acid, succinic acid or malic acid (Kanehisa and Goto 2000). According to

Fig. 3k, *L. plantarum* samples consume more aspartic acid than *L. rhamnosus,* and aspartic acid consumption increases at the high glucose concentration and the low pH_i value. For *L. rhamnosus* samples, only 'R5.5GH' samples consume considerable amount of aspartic acid, and at pH_i 6.5 samples, consumption of aspartic acid is very low.

3.5 Nucleosides and cell energy metabolism

Figure 3l shows the extracted kinetic profiles for adenosine. In our experiment, *L. plantarum* samples consume much more adenosine compared to *L. rhamnosus* samples. In all *L. plantarum* samples adenosine is depleted, which is not the case in *L. rhamnosus* samples (Fig. 3l). For *L. plantarum*, the rate of the adenosine consumption is higher in samples with high glucose concentration and the higher pH_i value, with glucose concentration having the main effect (Fig. 3l). The same glucose concentration dependence was observed for the *L. rhamnosus*. In 'R6.5GH' samples, adenosine is consumed at the same rate throughout the fermentation, but in 'R5.5GH' the rate of the adenosine consumption increases considerably after glucose depletion (Fig. 3l). *L. rhamnosus* samples with low glucose concentration consume the least amount of adenosine among all the other samples. Adenosine can be converted to inosine by adenosine deaminase (ADD, [EC: 3.5.4.4]) or to adenine by purine nucleoside phosphorylase (PNP, [EC: 2.4.2.1]). As Fig. 3m shows, inosine is only produced in *L. rhamnosus* samples, and analysis of the genome sequences from *L. plantarum* indicates that ADD is missing in these species (Kanehisa and Goto 2000). The maximum amount of inosine is formed in 'R5.5GH' samples (Fig. 3m). Figure 3n shows the kinetic profiles of adenine. Based on KEGG, PNP that can synthesize adenine from adenosine is present in both of the strains (Kanehisa and Goto 2000). It is observed that adenine is synthesized in the samples, and the patterns of its profiles are similar but inversed relative to the shape of the corresponding adenosine profiles. Overall, *L. plantarum* samples have a higher rate of adenine synthesis, and the highest amount of adenine is accumulated in 'P6.5GL' and 'P5.5GL' samples (Fig. 3n). In these samples, the concentration of adenine increases till the end of glucose depletion, but declines afterwards, especially in one of the 'P6.5GH' samples. Amongst the *L. rhamnosus* samples, the highest amount of adenine is synthesized in 'R5.5GH'. In 'R6.5GH', the concentration of adenine decreases till the end of glucose depletion, but starts to rise afterwards (Fig. 3n). As seen in Fig. 3l, n, *L. plantarum* consumes all the adenosine present in the CDIM medium and produces adenine, but no inosine. This is consistent with the presence of adenosine hydrolase [EC: 3.2.2.7], but the absence of adenosine deaminase [EC: 3.5.4.4] in *L. plantarum*. The hydrolase

activity appears to follow the bacterial concentration (OD value) and not to be dependent upon the growth rate of the bacteria. The accumulated adenine is not converted into adenosine monophosphate (AMP) by the adenine phosphoribosyl transferase (APRTase, [EC: 2.4.2.7]) or to hypoxanthine by the adenine deaminase [EC: 3.5.4.2] that is present in the bacterium. One explanation could be that adenine is exported into the medium. In *L. rhamnosus*, conversion of adenosine is much slower, though this bacterium has both adenosine hydrolase and adenosine deaminase. It is observed that both adenosine and inosine are accumulated during growth, but the speed of accumulation does not correlate with the growth rate. It appears as if the increased speed of adenosine consumption after 15 h with the 'R5.5GH' cultures coincided with decreased accumulation rate of both adenine and inosine, suggesting that inosine and adenine were both consumed for nucleotide synthesis through the salvage pathway.

3.6 Experimental design and significant factors

In order to investigate the significance of the experimental design factors, and to analyze some of the effect matrices, ASCA was applied on the extracted metabolic profiles including the OD profiles. Figure 4 shows the workflow for the data analysis and the ASCA results. As glucose was one of the experimental design factors and lactate production is highly correlated to the glucose consumption, these two metabolites were excluded prior to ASCA, in order to focus on the variation of the other metabolites. Based on the *p*-values of the effect matrices in Fig. 4, all the design factors, strains, pH, and glucose concentrations are statistically highly significant. The preliminary ASCA results showed that the *p*-values for the variance that is related to the replicates were not significant, as can be expected for a correctly performed experiment. Therefore, in the final ASCA, replicates were not included as the design factors. The *p*-values verify the experimental design and the experimental work.

The matrices that represent the strain related and pH related variances of the dataset were constructed by adding the residual matrix to the corresponding effect matrix that is given by ASCA, and were subsequently autoscaled and analyzed by PCA. Figure 5a shows the scores and the loadings biplot of the PCA analysis of the ASCA separated strains effect matrix. The first loading mainly describes consumption of adenosine, glutamine, and aspartic acid, and the concomitant production of acetic acid and adenine. The second loading mainly describes production of inosine, pyruvate, α-acetolactate, and formic acid. The PCA biplot shows that both *L. rhamnosus* and *L. plantarum* can metabolize adenosine, glutamine, and aspartic acid, but *L. plantarum* consumes them more. Furthermore, *L. plantarum* can produce more acetate and adenine, whereas, *L.*
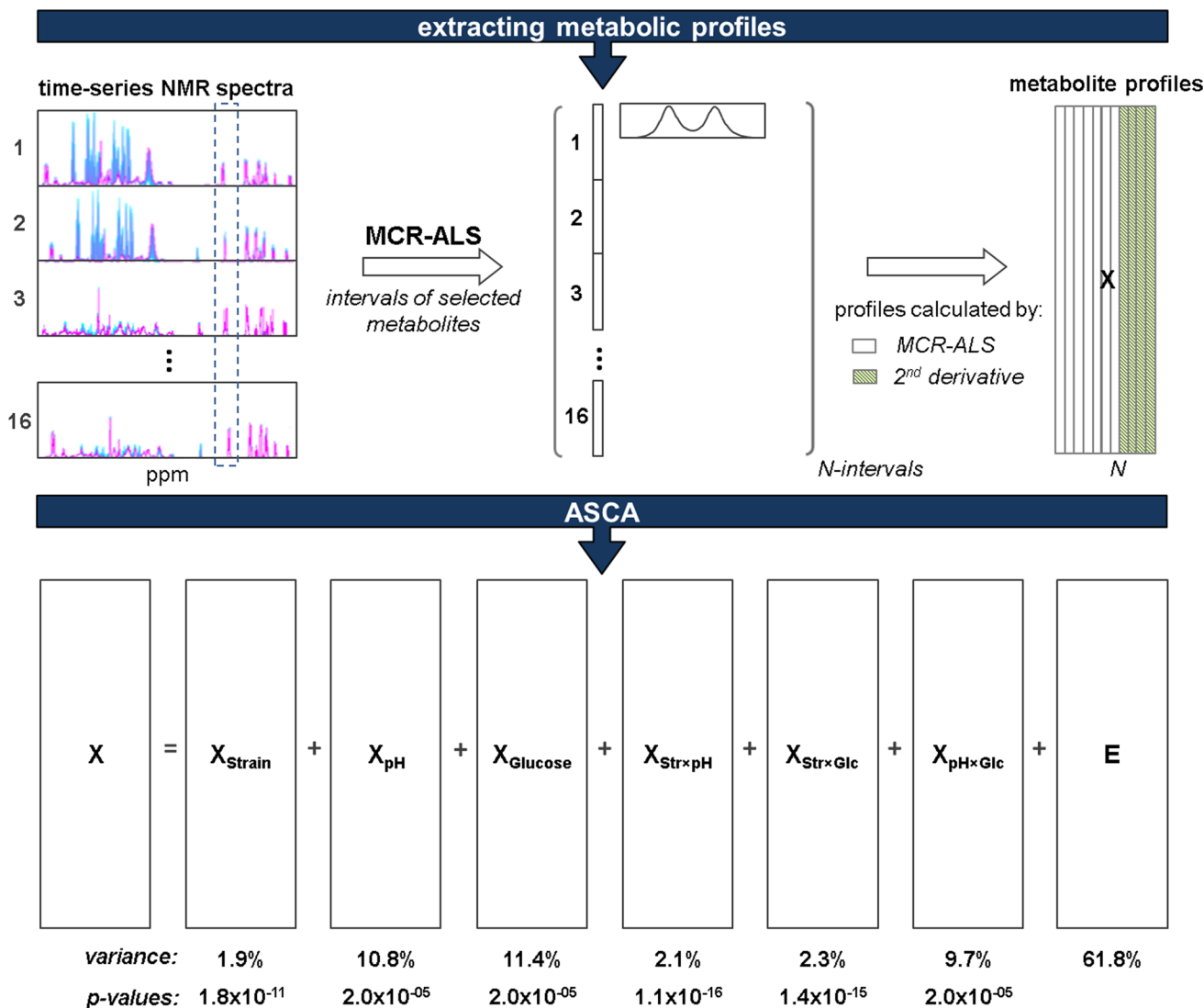
Fig. 4 The workflow for extracting the metabolic profiles by MCR-ALS and subsequent ASCA analysis. Some of the profiles were extracted by 2nd derivative approach. The explained variance and the p-values of the ASCA effect matrices are shown. 'X_{Strain}', 'X_{pH}', and '$X_{Glucose}$' are the main effect matrices of the corresponding design factors. '$X_{Str \times pH}$' and '$X_{Str \times Glc}$' are the strain-pH and strain-glucose interaction effect matrices, and '$X_{pH \times Glc}$' is the pH-glucose interaction effect matrix

rhamnosus can produce more inosine, pyruvate, acetolactate, and formic acid. This information was presented in a more segmented, but detailed manner by the extracted profiles, but the PCA results of the ASCA separated strain effect matrix, provides a more general and comprehensive overview of the strains differences in terms of the productions and consumption of the metabolites.

Figure 5b shows the PCA results of the pH separated effect matrix. For samples with pH_i 6.5, the end points of the fermentation mainly lead towards pyruvate and acetate, and for the samples with pH_i 5.5, towards α-acetolactate, adenine, formate, and inosine. As observed from this plot, aspartate consumption increases at pH_i 5.5 than at pH_i 6.5, whereas consumption of adenosine and glutamine

decrease. Figure 3S (the Online Resource) shows the PCA results of the strain specific pH effect matrix (the interaction between strain and pH).

The strain specific pH effect matrix (the interaction between the strains and pH_i) was also analyzed by PCA. The resulting scores and loadings plots are presented in Fig. 3S (the Online Resource). In the scores plot, only samples with the high glucose concentration are shown, because the samples with the lower glucose concentration are not influenced by the pH change as much as the samples with the higher glucose concentrations. The combination of the first and the third PCs show the fermentation trajectories of the two strains and how they are affected by the change in pH_i. The strains follow quite different
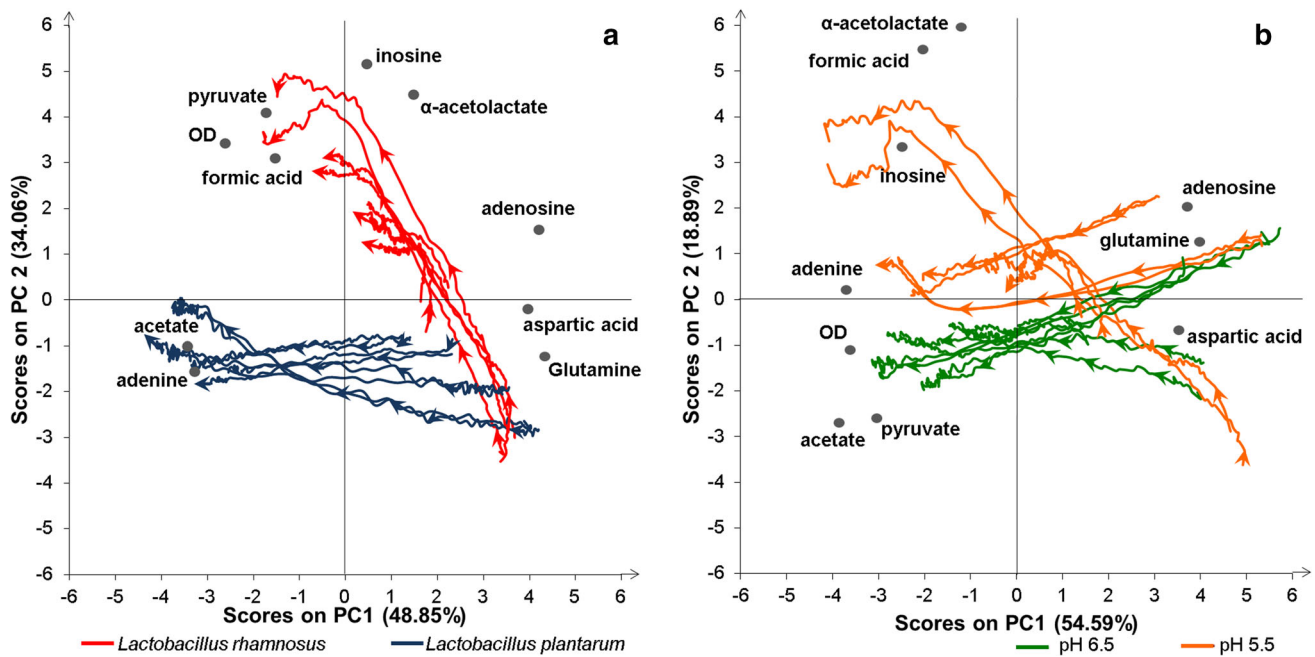
Fig. 5 PCA results of the ASCA effect matrices: **a** strains effect matrix, **b** pH effect matrix. The *arrows* on the scores trajectories show the time progression

trajectories at the same pH_i value, and also the metabolic shift in their metabolism due to the change in the pH_i is different. The perturbation in *L. rhamnosus* fermentation by pH_i change is more pronounced than in the *L. plantarum*, as the metabolic shift from 'R6.5GH' to 'R5.5GH' is stronger than the shift from 'P6.5GH' to 'P5.5GH'.

3.7 Pearson correlations and metabolite–metabolite heat maps

Figure 4S (the Online Resource) shows the correlation between the metabolites as heat maps, calculated as described in Sect. 2.3.2. These maps show which metabolites are highly correlated during the fermentation process. Table 1S shows number of the positive correlations that are bigger than 0.8 and the negative correlations that are smaller than −0.8, for all the samples. For *L. rhamnosus* samples with the higher glucose concentration, the numbers of the positive and negative correlations are increased considerably by the change of the pH_i from 6.5 to 5.5. This means that the change in the pH can significantly alter the metabolic state of the *L. rhamnosus* samples with the higher glucose concentration and by the decrease in pH, the concentration of more metabolites will decrease or increase concordantly, to reach a new metabolic equilibrium. This probably will help the cells to deal with the exerted pH stress. For *L. plantarum* samples with the high glucose concentration, the numbers of the positive and negative correlations decrease slightly at pH_i 5.5 compared

to pH_i 6.5. However, this level of perturbation in the metabolism is not comparable to the change that is observed in the corresponding *L. rhamnosus* samples. Therefore, it can be concluded that the metabolism of *L. rhamnosus* is more sensitive to pH decrease than the metabolism of *L. plantarum*. For *L. rhamnosus* and *L. plantarum* samples with the lower glucose concentration, the numbers of the positive and negative correlations between the metabolites are smaller compared to the samples with the higher glucose concentration. The numbers do not change between the two pH_i values. This may be due to the fact that the concentration of glucose in these samples is too low for the metabolism to reach equilibrium, and therefore the cells, being under the shortage of the carbohydrate source, cannot respond to the pH stress by shifting to a new metabolic state.

4 Concluding remarks

An efficient analytical protocol was developed for in vitro NMR studies of bacterial metabolism, from sample preparation to kinetic observation of metabolic changes. The protocol was successfully applied to an experimental design involving two LAB strains, two pH values and two initial glucose levels, where all the design factors proved to be highly significant and led to interesting biological information. One of the interesting biological findings was the different patterns of glutamine consumption by the two

strains. As glutamine plays a role in the catabolism of amino acids, augmenting its consumption can benefit the catabolism of amino acids, and consequently enhance the sensory properties of food products. Using the developed protocol, NMR proved to be an excellent analytical platform for real-time investigation of the gross details of bacterial metabolism. As for the data processing, reference deconvolution proved to be a necessary and elegant solution to the inherent inhomogeneity of in vitro NMR measurements of cells. It is recommended that reference deconvolution should be considered as a standard tool to enhance lineshapes and improve multivariate analysis results. The protocol can be used for studying different aspects of bacterial metabolism, and allows relatively easy investigation of different fermentation factors such as new strains, cohabitations, new substrates and deleterious metabolites, as well as temperature and pH.

References

Amarita, F., Requena, T., Taborda, G., Amigo, L., & Pelaez, C. (2001). *Lactobacillus casei* and *Lactobacillus plantarum* initiate catabolism of methionine by transamination. *Journal of Applied Microbiology, 90*, 971–978.

Annou, S., Maqueda, M., Martínez-Bueno, M., & Valdivia, E. (2007). Biopreservation, an ecological approach to improve the safety and shelf-life of foods. *Applied Microbiology, 1*, 475–486.

Aunsbjerg, S., Honoré, A., Vogensen, F., & Knøchel, S. (2015). Development of a chemically defined medium for studying foodborne bacterial–fungal interactions. *International Dairy Journal, 45*, 48–55.

Boroujerdi, A. F. B., Vizcaino, M. I., Meyers, A., Pollock, E. C., Huynh, S. L., Schock, T. B., et al. (2009). NMR-based microbial metabolomics and the temperature-dependent coral pathogen *vibrio coralliilyticus*. *Environmental Science and Technology, 43*, 7658–7664.

Caspi, R., Altman, T., Billington, R., Dreher, K., Foerster, H., Fulcher, C. A., et al. (2014). The MetaCyc database of metabolic pathways and enzymes and the BioCyc collection of Pathway/Genome Databases. *Nucleic Acids Research, 42*, D459–D471.

de Juan, A., Jaumot, J., & Tauler, R. (2014). Multivariate Curve Resolution (MCR). Solving the mixture analysis problem. *Analytical Methods, 6*, 4964–4976.

Delavenne, E., Ismail, R., Pawtowski, A., Mounier, J., Barbier, G., & Le Blay, G. (2013). Assessment of lactobacilli strains as yogurt bioprotective cultures. *Food Control, 30*, 206–213.

Delort, A.-M., Gaudet, G., & Forano, E. (2002). ^{23}Na NMR study of *Fibrobacter succinogenes* S85: Comparison of three chemical shift reagents and calculation of sodium concentration using ionophores. *Analytical Biochemistry, 306*, 171–180.

Delort, A.-M., Gaudet, G., & Forano, E. (2004). The use of chemical shift reagents and ^{23}Na NMR to study sodium gradients in microorganisms. *Environmental microbiology* (pp. 389–405). New York: Springer.

Ebrahimi, P., Nilsson, M., Morris, G. A., Jensen, H. M., & Engelsen, S. B. (2014). Cleaning up NMR spectra with reference deconvolution for improving multivariate analysis of complex mixture spectra. *Journal of Chemometrics, 28*, 656–662.

Emwas, A. H. M., Salek, R. M., Griffin, J. L., & Merzaban, J. (2013). NMR-based metabolomics in human disease diagnosis: Applications, limitations, and recommendations. *Metabolomics, 9*, 1048–1072.

Engelsen, S. B., Savorani, F., & Rasmussen, M. A. (2013). Chemometric exploration of quantitative NMR data. eMagRes. Wiley. doi:10.1002/9780470034590.emrstm1304.

Fernández, M., & Zúñiga, M. (2006). Amino acid catabolic pathways of lactic acid bacteria. *Critical Reviews in Microbiology, 32*, 155–183.

Govindaraju, V., Young, K., & Maudsley, A. A. (2000). Proton NMR chemical shifts and coupling constants for brain metabolites. *NMR in Biomedicine, 13*, 129–153.

Grivet, J. P., & Delort, A. M. (2009). NMR for microbiology: In vivo and in situ applications. *Progress in Nuclear Magnetic Resonance Spectroscopy, 54*, 1–53.

Grivet, J.-P., Delort, A.-M., & Portais, J.-C. (2003). NMR and microbiology: From physiology to metabolomics. *Biochimie, 85*, 823–840.

Helinck, S., Le Bars, D., Moreau, D., & Yvon, M. (2004). Ability of thermophilic lactic acid bacteria to produce aroma compounds from amino acids. *Applied and Environmental Microbiology, 70*, 3855–3861.

Hung, Y. P., Albeck, J. G., Tantama, M., & Yellen, G. (2011). Imaging cytosolic NADH–NAD^{+} redox state with a genetically encoded fluorescent biosensor. *Cell Metabolism, 14*, 545–554.

Hung, Y. P., & Yellen, G. (2014). Live-cell imaging of cytosolic NADH–NAD^{+} redox state using a genetically encoded fluorescent biosensor. *Fluorescent protein-based biosensors* (pp. 83–95). New York: Springer.

Jaumot, J., Gargallo, R., de Juan, A., & Tauler, R. (2005). A graphical user-friendly interface for MCR-ALS: A new tool for multivariate curve resolution in MATLAB. *Chemometrics and Intelligent Laboratory Systems, 76*, 101–110.

Kanehisa, M., & Goto, S. (2000). KEGG: Kyoto encyclopedia of genes and genomes. *Nucleic Acid Research, 28*, 27–30.

Kieronczyk, A., Skeie, S., Langsrud, T., & Yvon, M. (2003). Cooperation between *Lactococcus lactis* and nonstarter lactobacilli in the formation of cheese aroma from amino acids. *Applied and Environmental Microbiology, 69*, 734–739.

Kieronczyk, A., Skeie, S., Olsen, K., & Langsrud, T. (2001). Metabolism of amino acids by resting cells of non-starter lactobacilli in relation to flavour development in cheese. *International Dairy Journal, 11*, 217–224.

Kilstrup, M., Hammer, K., Jensen, P. R., & Martinussen, J. (2005). Nucleotide metabolism and its control in lactic acid bacteria. *FEMS Microbiology Reviews, 29*, 555–590.

Kim, H. K., Choi, Y. H., & Verpoorte, R. (2010). NMR-based metabolomic analysis of plants. *Nature Protocols, 5*, 536–549.

Kim, H. K., Choi, Y. H., & Verpoorte, R. (2011). NMR-based plant metabolomics: Where do we stand, where do we go? *Trends in Biotechnology, 29*, 267–275.

Kim, Y. S., Maruvada, P., & Milner, J. A. (2008). Metabolomics in biomarker discovery: Future uses for cancer prevention. *Future Oncology, 4*, 93–102.

Koebmann, B. J., Andersen, H. W., Solem, C., & Jensen, P. R. (2002). Experimental determination of control of glycolysis in *Lactococcus lactis*. *Antonie van Leeuwenhoek, 82*, 237–248.

Kowalczyk, M., & Bardowski, J. (2007). Regulation of sugar catabolism in *Lactococcus lactis*. *Critical Reviews in Microbiology, 33*, 1–13.

Kumari, A., Catanzaro, R., & Marotta, F. (2011). Clinical importance of lactic acid bacteria: A short review. *Acta bio-medica: Atenei Parmensis, 82*, 177–180.

Lahtinen, S., Ouwehand, A. C., Salminen, S., & von Wright, A. (2011). *Lactic acid bacteria: Microbiological and functional aspects*. Boca Raton: CRC Press.

Lankadurai, B. P., Nagato, E. G., & Simpson, M. J. (2013). Environmental metabolomics: An emerging approach to study organism responses to environmental stressors. *Environmental Reviews, 21*, 180–205.

Larive, C. K., Barding, G. A, Jr, & Dinges, M. M. (2014). NMR spectroscopy for metabolomics and metabolic profiling. *Analytical Chemistry, 87*, 133–146.

Lawton, W. H., & Sylvestre, E. A. (1971). Self modeling curve resolution. *Technometrics, 13*(3), 617–633.

Le Bars, D., & Yvon, M. (2008). Formation of diacetyl and acetoin by *Lactococcus lactis* via aspartate catabolism. *Journal of Applied Microbiology, 104*, 171–177.

Liu, M., Nauta, A., Francke, C., & Siezen, R. J. (2008). Comparative genomics of enzymes in flavor-forming pathways from amino acids in lactic acid bacteria. *Applied and Environmental Microbiology, 74*, 4590–4600.

Ljungh, A., & Wadström, T. (2006). Lactic acid bacteria as probiotics. *Current Issues in Intestinal Microbiology, 7*, 73–90.

Marin-Valencia, I., Yang, C., Mashimo, T., Cho, S., Baek, H., Yang, X.-L., et al. (2012). Analysis of tumor metabolism reveals mitochondrial glucose oxidation in genetically diverse human glioblastomas in the mouse brain in vivo. *Cell Metabolism, 15*, 827–837.

Martini, S., Ricci, M., Bartolini, F., Bonechi, C., Braconi, D., Millucci, L., et al. (2006). Metabolic response to exogenous ethanol in yeast: An in vivo NMR and mathematical modelling approach. *Biophysical Chemistry, 120*, 135–142.

Martini, S., Ricci, M., Bonechi, C., Trabalzini, L., Santucci, A., & Rossi, C. (2004). In vivo ^{13}C-NMR and modelling study of metabolic yield response to ethanol stress in a wild-type strain of *Saccharomyces cerevisiae*. *FEBS Letters, 564*, 63–68.

Mashego, M. R., Rumbold, K., De Mey, M., Vandamme, E., Soetaert, W., & Heijnen, J. J. (2007). Microbial metabolomics: Past, present and future methodologies. *Biotechnology Letters, 29*, 1–16.

Morris, G. A. (2007). Reference Deconvolution. *eMagRes*. Wiley. doi:10.1002/9780470034590.emrstm0449.

Morris, G. A., Barjat, H., & Home, T. J. (1997). Reference deconvolution methods. *Progress in Nuclear Magnetic Resonance Spectroscopy, 31*, 197–257.

Neves, A. R., Pool, W. A., Kok, J., Kuipers, O. P., & Santos, H. (2005). Overview on sugar metabolism and its control in *Lactococcus lactis*—The input from in vivo NMR. *FEMS Microbiology Reviews, 29*, 531–554.

Neves, A. R., Ramos, A., Nunes, M. C., Kleerebezem, M., Hugenholtz, J., de Vos, W. M., et al. (1999). *In vivo* nuclear magnetic resonance studies of glycolytic kinetics in *Lactococcus lactis*. *Biotechnology and Bioengineering, 64*, 200–212.

Nicholson, J. K., Holmes, E., Kinross, J., Burcelin, R., Gibson, G., Jia, W., & Pettersson, S. (2012). Host-gut microbiota metabolic interactions. *Science, 336*, 1262–1267.

Nicholson, J. K., & Lindon, J. C. (2008). Systems biology: Metabonomics. *Nature, 455*, 1054–1056.

Nilsson, M. (2009). The DOSY Toolbox: A new tool for processing PFG NMR diffusion data. *Journal of Magnetic Resonance, 200*, 296–302.

Ramos, A., Neves, A. R., & Santos, H. (2002). Metabolism of lactic acid bacteria studied by nuclear magnetic resonance. In *Lactic acid bacteria: Genetics, metabolism and applications* (pp. 249–261). Springer.

Reo, N. V. (2002). NMR-based metabolomics. *Drug and Chemical Toxicology, 25*, 375–382.

Ricci, M., Aggravi, M., Bonechi, C., Martini, S., Aloisi, A. M., & Rossi, C. (2012). Metabolic response to exogenous ethanol in yeast: An in vivo statistical total correlation NMR spectroscopy approach. *Journal of Biosciences, 37*, 749–755.

Rothman, D. L., Behar, K. L., Hyder, F., & Shulman, R. G. (2003). In vivo NMR studies of the glutamate neurotransmitter flux and neuroenergetics: Implications for brain function. *Annual Review of Physiology, 65*, 401–427.

Rueedi, R., Ledda, M., Nicholls, A. W., Salek, R. M., Marques-Vidal, P., Morya, E., et al. (2014). Genome-wide association study of metabolic traits reveals novel gene-metabolite-disease links. *PLoS Genetics, 10*, e1004132.

Savorani, F., Tomasi, G., & Engelsen, S. B. (2010). *i*coshift: A versatile tool for the rapid alignment of 1D NMR spectra. *Journal of Magnetic Resonance, 202*, 190–202.

Sekiyama, Y., Chikayama, E., & Kikuchi, J. (2011). Evaluation of a semipolar solvent system as a step toward heteronuclear multidimensional NMR-based metabolomics for ^{13}C-labeled bacteria, plants, and animals. *Analytical Chemistry, 83*, 719–726.

Serrazanetti, D. I., Guerzoni, M. E., Corsetti, A., & Vogel, R. (2009). Metabolic impact and potential exploitation of the stress reactions in lactobacilli. *Food Microbiology, 26*, 700–711.

Siegumfeldt, H., Rechinger, K. B., & Jakobsen, M. (2000). Dynamic changes of intracellular pH in individual lactic acid bacterium cells in response to a rapid drop in extracellular pH. *Applied and Environmental Microbiology, 66*, 2330–2335.

Smilde, A. K., Jansen, J. J., Hoefsloot, H. C., Lamers, R.-J. A., Van Der Greef, J., & Timmerman, M. E. (2005). ANOVA-simultaneous component analysis (ASCA): A new tool for analyzing designed metabolomics data. *Bioinformatics, 21*, 3043–3048.

Smolinska, A., Blanchet, L., Buydens, L. M., & Wijmenga, S. S. (2012). NMR and pattern recognition methods in metabolomics: From data acquisition to biomarker discovery: A review. *Analytica Chimica Acta, 750*, 82–97.

Sun, F., Dai, C., Xie, J., & Hu, X. (2012). Biochemical issues in estimation of cytosolic free NAD$^+$/NADH ratio. *PLoS One, 7*, e34525.

Tanous, C., Kieronczyk, A., Helinck, S., Chambellon, E., & Yvon, M. (2002). Glutamate dehydrogenase activity: A major criterion for the selection of flavour-producing lactic acid bacteria strains. *Lactic acid bacteria: Genetics, metabolism and applications* (pp. 271–278). Berlin: Springer.

Ulrich, E. L., Akutsu, H., Doreleijers, J. F., Harano, Y., Ioannidis, Y. E., Lin, J., et al. (2008). BioMagResBank. *Nucleic Acids Research, 36*, D402–D408.

van de Guchte, M., Serror, P., Chervaux, C., Smokvina, T., Ehrlich, S. D., & Maguin, E. (2002). Stress responses in lactic acid bacteria. *Antonie van Leeuwenhoek, 82*, 187–216.

Wang, H., Tso, V. K., Slupsky, C. M., & Fedorak, R. N. (2010). Metabolomics and detection of colorectal cancer in humans: A systematic review. *Future Oncology, 6*, 1395–1406.

Williams, A. G., Noble, J., & Banks, J. M. (2001). Catabolism of amino acids by lactic acid bacteria isolated from Cheddar cheese. *International Dairy Journal, 11*, 203–215.

Winning, H., Larsen, F. H., Bro, R., & Engelsen, S. B. (2008). Quantitative analysis of NMR spectra with chemometrics. *Journal of Magnetic Resonance, 190*, 26–32.

Wishart, D. S. (2008). Quantitative metabolomics using NMR. *TrAC Trends in Analytical Chemistry, 27*, 228–237.

Wishart, D. S., Jewison, T., Guo, A. C., Wilson, M., Knox, C., Liu, Y., et al. (2012). HMDB 3.0—The human metabolome database in 2013. *Nucleic Acids Research, 41*(Database issue), D801–D807.

Wishart, D. S., Knox, C., Guo, A. C., Eisner, R., Young, N., Gautam, B., et al. (2009). HMDB: A knowledgebase for the human metabolome. *Nucleic Acids Research, 37*, D603–D610.

Wishart, D. S., Tzur, D., Knox, C., Eisner, R., Guo, A. C., Young, N., et al. (2007). HMDB: The human metabolome database. *Nucleic Acids Research, 35*, D521–D526.